NHC-Stabilized Germaacylium ion: Reactivity and Utility in Catalytic CO_2 Functionalizations

Debotra Sarkar,[†] Catherine Weetman,[†] Sayan Dutta,[‡] Emeric Schubert,[†] Christian Jandl,[†] Debasis Koley,[*,‡] and Shigeyoshi Inoue[*,†]

[†]Department of Chemistry, WACKER-Institute of Silicon Chemistry and Catalysis Research Center, Technische Universität München, Lichtenbergstraße 4, 85748 Garching, Germany

[‡]Department of Chemical Sciences, Indian Institute of Science Education and Research (IISER) Kolkata, Mohanpur 741 246, India.

KEYWORDS: NHC, Main Group, Germanium, Oxides, Cations, CO_2 conversion, Catalysis, DFT

ABSTRACT: The first acceptor-free heavier germanium analogue of an acylium ion, $[RGe(O)(NHC)_2]X$ (R = ^{Mes}Ter= 2,6-(2,4,6-$Me_3C_6H_2)_2C_6H_3$; NHC = IMe_4 = 1,3,4,5-tetramethylimidazol-2-ylidene; X = (Cl or BArF= {(3,5–$(CF_3)_2C_6H_5)_4B$}), was isolated by reacting $[RGe(NHC)_2]X$ with N_2O. Conversion of the germa-acylium ion to the first solely donor-stabilized germanium ester $[(NHC)RGe(O)(OSiPh_3)]$ and corresponding heavier analogues ($[RGe(S)(NHC)_2]X$ and $[RGe(Se)(NHC)_2]X$) demonstrated its classical acylium-like behavior. The polarized terminal GeO bond in the germa-acylium ion was utilized to activate CO_2 and silane, with the former found to be an example of reversible activation of CO_2, thus mimicking the behavior of transition metal oxides. Furthermore, its transition metal like nature is demonstrated as it was found to be an active catalyst in both CO_2 hydrosilylation and reductive *N*-functionalization of amines using CO_2 as C_1 source. Mechanistic studies were undertaken both experimentally and computationally, which revealed the reaction proceeds via a NHC-siloxygermylene $[(NHC)RGe(OSiHPh_2)]$.

INTRODUCTION

The catalytic conversion of CO_2 into useful commodity chemicals has drawn considerable attention in the last decades, due to the increasing global energy demands and concomitant rising CO_2 emissions.[1-5] CO_2 is chemically abundant and finds use as a C_1 building block. Albeit, these transformations are challenging due to the high C-O bond strength in CO_2 (552 kJ mol-1).[3-4, 6] Pertinent to this work, the catalytic hydrosilylation of CO_2 to corresponding silyl formate, acetals, silyl ether, and methane presents an attractive route for CO_2 utilization. The inherent stability of Si–O bond and the propensity behind Si–H bond scission to form metal hydrides result in the exergonic nature of hydrosilylation vs. hydrogenation. Furthermore, the high natural abundance of silicon makes it an ideal candidate for transformation of CO_2 into commodity chemicals.[3, 6-7] As an extension to hydrosilylation of CO_2, the "diagonal approach" provides an alternative method for CO_2 utilization, as the combination of CO_2 and silanes provides the C_1 source for *N*-formylation or *N*-methylation of amines.[8] Recently, transition metal oxides (TMOs) in high oxidation states have shown potenial application in reductive CO_2 derivatisation.[9-14] For example, high valent rhenium and tungsten oxo-anions are active catalysts in the hydrosilylation of CO_2.[13-14] In this context, theoretical studies revealed the formation of a hypercoordinate silicate to be key in enabling turnover, as reduction of CO_2 occurs at the activated Si-H bond (Figure 1a).[13] In contrast, catalysis by cationic rhenium-oxides catalysts proceeds via rhenium hydrides, as silane adds across the Re=O double bond forming Re-H intermediates which are responsible for the resulting CO_2 reduction to silyl formate (Figure 1b).[15]

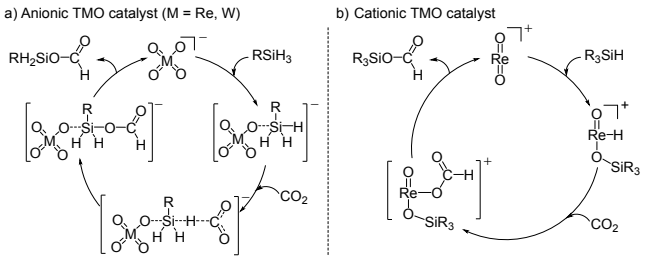

Figure 1. Activation of CO_2 with both anionic (a) and cationic (b) transition metal oxides.

Recent years have seen a growing interest in main group elements ability to mimic transition metals, due to main group elements being more advantageous from both an economic and environmental point of view.[16-19] In this regard, heavier group-14 terminal oxides, [E=O] (E = Si, Ge, Sn), could provide an alternative to high oxidation state TMOs.[20] Similar to TMOs,[10] germanone (R_2GeO)[21] and silanone (R_2SiO)[22-25] readily undergo [2+2]-cycloaddition with CO_2 to form metal carbonates, as a result of the polarized E=O bond.[20] Interestingly, Si=O bond mediated reversible cycloaddition of CO_2 has recently been demonstrated by Kato and co-workers.[26] It is also of note that group 13 molecular oxides have been found to activate CO_2, also due to the highly polarized Al-O

bond. This has been shown by both terminal aluminium oxide ions $[R_2AlO]^-$[27-28] and by a dimeric $[R_2AlO]_2$ complex.[29] However, to the best of our knowledge, the only example of further functionalization of either a group 13 or 14 carbonate to value-added products was reported by our group.[29] Where an aluminium double bond was found to selectively catalyze the reduction of CO_2 to a formic acid equivalent, with a dialuminium carbonate pivotal to the calculated mechanism. Beyond the sequestration of CO_2, an elegant study by Driess and co-workers illustrated the activation of ammonia (NH_3) with the polar Si=O bond, which strongly resembles transition metal reactivity.[30] Moreover, activation of E'-H bonds (E' = O, Si, C) has also been achieved by R_2EO complexes (E = Si, Ge).[21-23, 31] Despite these successes, the catalytic application of these oxides has not yet been explored. One of the potential difficulties in employing heavier group 14 oxides is the inherent thermodynamic instability of these complexes. The tendency to oligomerize is attributed to the highly zwitterionic nature of the E-O bond, therefore, rational steric and electronic stabilization is required to address such a challenge.[20] Additionally, hydrosilylation reactions also pose their own challenges due to their propensity to form stable metal-oxosilyl complexes. These compounds have a formal oxidation state of +4 and are highly stable species. This makes traditional redox-based catalysis very challenging due to the difficulties associated with reductive elimination and, therefore, release of the functionalized substrate.[21-23, 31]

One potential method to overcome this difficulty is to use a metal center which is stable in both high and low oxidation states, thus, germanium presents itself as an ideal candidate. In recent years the transition metal like ability of germanium has been shown providing the first examples of low-valent main group dihydrogen activation and multiple bond catalysis.[32-40] With the latter example possible due to the ability of germanium to switch between its +2 and +4 oxidation states. With these incentives in mind, we targeted the synthesis of a Lewis base stabilized germanium oxide ion, the elusive heavier analog of an acylium ion, and to examine its application in CO_2 functionalization. In order to access such a species, we envisaged that N-heterocyclic carbenes (NHC)-stabilized germyliumylidenes,[41-42] would provide the necessary steric and electronic requirements to provide access to the germa-acylium ion. Notably, $[R\text{-}GeO]^+$ are transient species, having only been detected by using high pressure and Fourier transformation mass spectrometry (FTMS).[43]

Scheme 1. Synthesis of NHC-stabilized germyliumylidene ion 2[Cl], germa-acylium ion 3[X] and possible resonance structure of 3[X] (X = Cl, BArF).

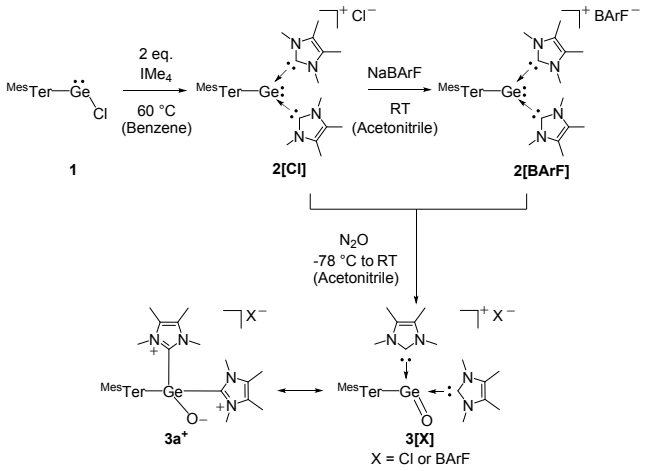

RESULTS AND DISCUSSION

The NHC-stabilized germyliumylidene (**2[Cl]**, ^{Mes}TerGe(IMe$_4$)$_2$]Cl, ^{Mes}Ter = 2,6-(2,4,6-Me$_3$C$_6$H$_2$)$_2$C$_6$H$_3$), was isolated by treating chlorogermylene (**1**, ^{Mes}TerGeCl) with two equivalents of IMe$_4$ (IMe$_4$ = 1,3,4,5-tetramethylimidazol-2-ylidene) in benzene at 60°C (Scheme 1). This led to the immediate precipitation of compound **2[Cl]**, as colorless needles which could be isolated in 84% yield. Compound **2[Cl]** is soluble in polar solvents such as acetonitrile and fluorobenzene but poorly soluble in nonpolar organic solvents. The solubility was improved by anion exchange. Treatment of compound **2[Cl]** with Na[BArF] (BArF = 3,5–(CF$_3$)$_2$C$_6$H$_5$)$_4$B) afforded **2[BArF]** (yield = 97%). Compounds **2[Cl]** and **2[BArF]** were both characterized by multinuclear NMR spectroscopy. In the ^{1}H and ^{13}C{^{1}H} NMR spectrum of **2[BArF]**, a characteristic signal for [BArF]- was observed at δ 7.40 ppm and δ 162.2 ppm (B-C, q, $^1J_{BC}$ = 50.0 Hz), respectively. This indicates successful counter anion exchange. For both compounds, the carbene carbon resonance was found at δ 164.0 ppm in the ^{13}C{^{1}H} NMR, which is in the range of NHC stabilized germyliumylidenes.[44-47]

Single crystal X-ray diffraction (SC-XRD) analysis revealed that the central germanium is tri-coordinate, with two NHCs and one m-terphenyl group coordinated (Figure 2). The Ge…Cl distance in **2[Cl]** is above 6 Å, indicating the absence of significant interactions between the germanium and chlorine atoms. The Ge-C^{NHC} bond distances in **2[Cl]** for the coordinated NHCs are almost identical 2.093(3) Å and 2.063(3) Å and are similar to the other NHC stabilized germyliumylidenes.[44-48] The optimized geometry of **2$^+$** calculated at the R/U-BP86/def2-SVP is in good agreement with the experimental data (see SI). Inspection of the frontier molecular orbitals reveal that the HOMO in **2$^+$** represents the σ-symmetric lone pair orbital located on the germanium center, whereas the LUMO possesses the π-symmetric vacant molecular orbital concentrated on the carbene carbons (Figure S50). Natural bond orbital (NBO) analysis suggests that the Ge–C^{NHC} bonds are significantly polarized towards the carbene carbon atoms (C25: 75.9%, C32: 76.4%). Furthermore, calculated Wiberg bond indices (WBI) of 0.735 and 0.723 support the single bond character of these bonds.

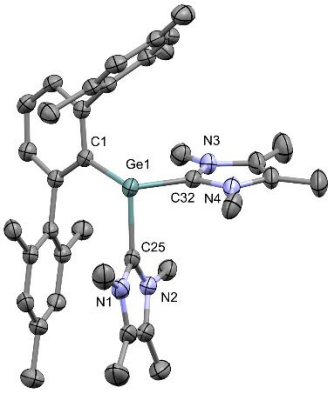

Figure 2. Molecular structures of compound **2[Cl]** in the solid state. Ellipsoids are set at the 50% probability level; hydrogen atoms and counter ion are omitted for clarity. Selected bond lengths [Å] and bond angles [°]: Ge1-C1 2.044(3), Ge1-C32 2.063(3), Ge1-C25 2.093(3), C1-Ge1-C25 109.02(12), C1-Ge1-C32 102.17(13), C32-Ge1-C25 91.36(12).

Since the electron rich germanium(II) can easily undergo for oxidative addition in presence of an oxidizing agent,[44, 49-51] this prompted us to treat compound **2** with an oxygen transfer reagent, e.g. N_2O, to target the isolation of a germaacylium ion. Indeed, treatment of compound **2** with N_2O (1 bar) led to the desired product, (**3**, ^{Mes}TerGe(O)$(IMe_4)_2$]X, X = Cl or BArF) in near quantitative yields (**3[Cl]** = 89% and **3[BArF]** = 94%, Scheme 1). The ^{1}H NMR spectrum of compound **3** displays two distinct broad signals (δ 3.21 and δ 4.20 ppm) which are assigned as the *N*-Methyl groups of the NHCs. Whilst in the ^{13}C{^{1}H} NMR spectrum, the carbene carbon resonance has shifted upfield from compound **2** (δ164.0 ppm to δ149.9 ppm), indicating strong interaction between Ge and the carbene carbon.

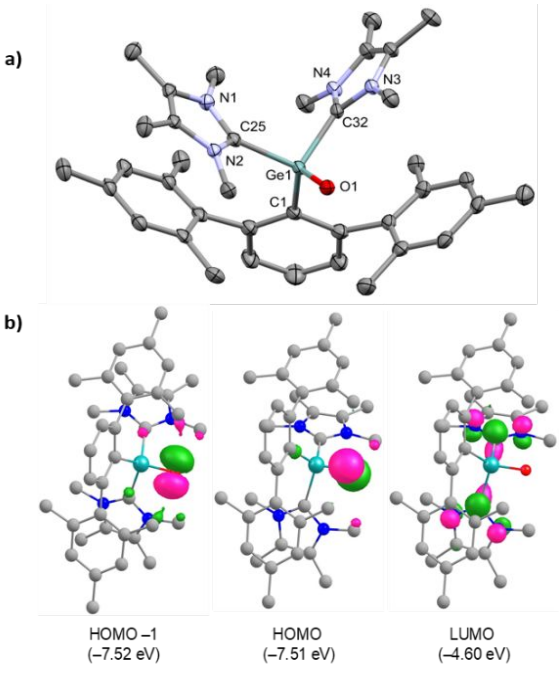

Figure 3. (a) Molecular structures of compound **3[BArF]** in the solid state. Ellipsoids are set at the 50% probability level; hydrogen atoms, counter ion and co-crystallized solvent molecules are omitted for clarity. Selected bond lengths [Å] and bond angles [°]: Ge1-O1 1.697(3), Ge1-C1 1.986(4), Ge1-C32 2.034(4), Ge1-C25 2.036(4), C1-Ge1-C32 104.88(15), C1-Ge1-C25 116.90(14), C32-Ge1-C25 104.30(15), O1-Ge1-C25 103.30(13), O1-Ge1-C32 109.26(13), O1-Ge1-C1 117.40(14). (b) Selected KS-MOs of **3**$^+$ (isosurface =0.07 a.u.). The orbital energies are shown in parentheses. Hydrogen atoms are omitted for clarity.

The molecular structure of complex **3[BArF]** was unambiguously confirmed by SC-XRD analysis (Figure 3a), which revealed a distorted tetrahedral geometry at the germanium center. The Ge-O bond in complex **3[BArF]** is 1.697(3) Å, which is shorter than a tetracoordinate Ge-O single bond (1.76-1.82 Å) and falls within the range of donor/acceptor stabilized germanones (1.673-1.718 Å).[49-53] This bond is relatively elongated compared to three coordinate germanone 1.646(5) Å.21 In the solid-state-IR spectrum compound **3** displays a strong absorption at 807 cm^{-1} which is assigned as Ge=O. This is blue shifted compared to the reported Ge=O stretching in $Eind_2Ge$=O (917 cm^{-1}), and red shifted in comparison to Ge-O single bond stretching frequency (769 cm^{-1}).[54] Thus, structural and IR data suggest a strong dominance of a zwitterionic resonance form (**3a**$^+$, Scheme 1) in the ground state. The calculated structure of **3**$^+$ is in good agreement with the experimental structure (calculated IR 800.8 cm^{-1}). Examination of the Ge-O bond by NBO and WBI analysis revealed a strong polarization towards the oxygen center (O1 78.9%) and a WBI value of 0.896, indicating single bond character. Additionally, the NPA charges (Ge +1.679 e and O -1.230 e) in **3**$^+$ further support the dominance of the zwitterionic resonance form **3a**$^+$. Inspection of the frontier orbitals show the HOMO-1 and HOMO in **3**$^+$ comprise of the lone pair orbitals on the O atom, whereas the LUMO consists of the vacant p_π orbital on the carbene carbons (Figure 3b).

Scheme 2. Reactivity of germa-acylium ion 3[X] (X= Cl, BArF, LR = Lawesson's Reagent $(CH_3OPhPS_2)_2$, WR = Wollin's reagents $(PhPSe_2)_2$, Dipp = 2,6-i$Pr_2C_6H_3$).

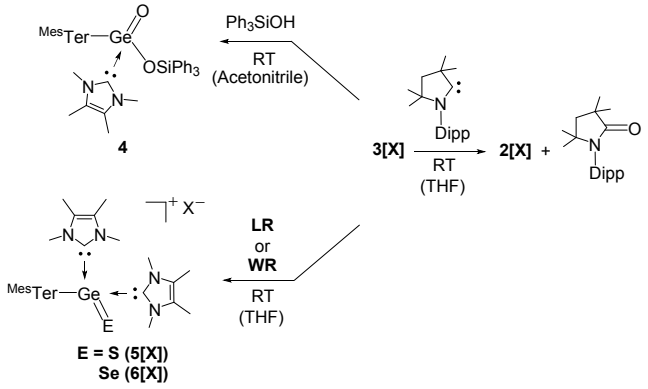

In order to examine a relationship to classical acyl transfer, we treated compound **3** with Ph_3SiOH, this resulted in the first example of an acceptor free stable germanium ester, compound **4**, [(^{Mes}TerGe(O)$(OSiPh_3)(IMe_4)$], with the concomitant formation of imidazolium salt (Scheme 2). Compound **4** was characterized by standard spectroscopic and analytic methods. In the ^{13}C{^{1}H} NMR the carbene carbon resonance was found at δ 153.2 ppm and a distinct silicon resonance at δ -19.3 ppm was observed in the ^{29}Si{^{1}H} NMR spectrum. SC-XRD analysis further confirmed the coordination of one NHC to the germanium center (Figure 4). In **4** the Ge1-O1 bond length is 1.682(16) Å, which is shorter than **3[BArF]** (1.697 (3) Å) as

well as the donor-acceptor stable germa-ester complex 1.719(2) Å, reported recently by Nagendran, and marginally longer than the NHC-stabilized germanone (1.670-1.672 Å) reported by Driess.[49, 52] Expectedly, the Ge1-O2 bond length (1.802(18) Å) is longer than Ge1-O1 bond and is more in line with typical Ge-O single bond values.[52-53] Theoretical studies suggest the formation of **4** proceeds via a stable intermediate which contains a strong hydrogen bond from the hydroxyl proton in Ph_3SiOH to the O1 center in **3M⁺**. Proton transfer to O1 then occurs, followed by de-coordination of IMe_4 which then allows for proton abstraction from O1 to deliver the desired germanium ester (Figure S52).

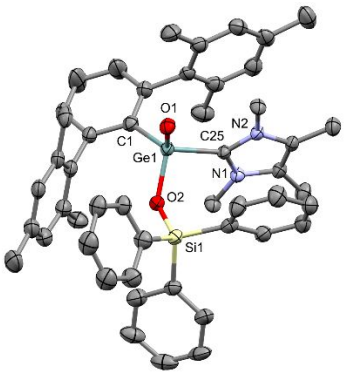

Figure 4. Molecular structures of compound **4** in the solid state (one out of two independent molecules in the asymmetric unit). Ellipsoids are set at the 50% probability level; hydrogen atoms and co-crystallized solvent molecules are omitted for clarity. Selected bond lengths [Å] and bond angles [°]: Ge1-O1 1.682(16), Ge1-O2 1.802(18), Ge1-C1 1.979(3), Ge1-C25 2.007(2), C1-Ge1-C25 109.45(10), C1-Ge1-O2 108.84(9), O1-Ge1-C1 115.64(10), O1-Ge1-O2 113.25(8), O1-Ge1-C25 110.45(9), O1-Ge1-C1 115.64(10), O2-Ge1-C25 97.72(9).

Recently we have demonstrated the sila-wittig reaction with silanone, for a range of substrates.[55] In which one of the driving forces of this reaction was the formation of stable P=O bonds. To access heavier germaaccylium analogs we envisaged the use of Lawesson's [LR = $(CH_3OPhPS_2)_2$] and Wollins reagents [WR = $(PhPSe_2)_2$], which are mild and convenient thionating and selanating reagents for ketones, esters, and amides which enable the preparation of thio- and seleno carbonyls, respectively.[56-57] Again, the driving force of these reactions is the formation of a stable P=O bond in a cycloreversion step that resembles the mechanism of Wittig reactions.[58] As such, we investigated the use of LR and WR with compound **3** (Scheme 2). Under ambient conditions, reaction of **3** with LR and WR afforded compounds [^{Mes}TerGe(S)$(IMe_4)_2$]X (**5**) and [^{Mes}TerGe(Se)$(IMe_4)_2$]X (**6**) in (**5[Cl]** = 39%, **5[BArF]** = 35%) and (**6[Cl]** = 30%, **6[BArF]** = 29%) yield, respectively. The Ge-S bond length in **5[BArF]** (2.104(7) Å) is close to those of donor stabilized Ge=S bonds (ranging from 2.053 to 2.095 Å) and shorter than the typical Ge-S single bond length (2.239 Å) (Figure 5).[46, 59-64] Similarly, the Ge-Se bond length in **6[BArF]** (2.237 (5) Å) is sufficiently shorter than a Ge-Se single bond (2.461 Å) and falls within the range of tetracoordinated donor stabilized Ge=Se bonds (Figure 5).[60-61] The Ge-S and Ge-Se bond in compound **5** and **6**, are longer than the kinetically stabilized tricoordinate Ge=S and Ge=Se bonds, respectively.[65] Notably, compound **6[BArF]** represents the first example of cationic germaselenium complex. NBO analyses on compounds **5⁺** and **6⁺** suggest that the Ge–Ch (Ch = O, S, Se) bond becomes less polarized in nature on descending the group (O: 78.9%, S: 60.5%, Se: 55.3%). Moreover, unlike the Ge–O bond in **3⁺**, Ge–S and Ge–Se bonds show partial double bond character, as supported by the calculated WBI values of 1.279 and 1.302, respectively. We have theoretically explored the reaction mechanism for the formation of **5**. Our calculations suggest the dissociation of the dimeric **LR** followed by the nucleophilic attack of O1 in **3M⁺** at the electron deficient phosphorus in the monomeric unit (**LR^M**) initiates the reaction (Figure S53).

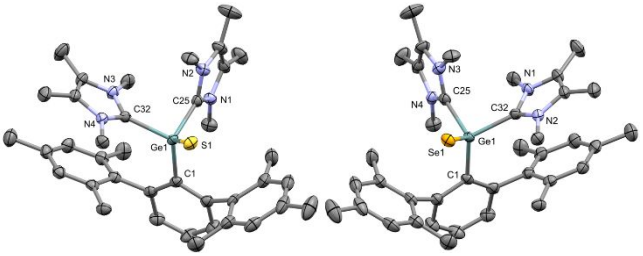

Figure 5. Molecular structure of compound **5[BArF]** (left) and **6[BArF]** (right) in the solid state. Ellipsoids are set at the 50% probability level; hydrogen atoms, counter ions and co-crystallized solvent molecules are omitted for clarity. Selected bond lengths [Å]and bond angles [°]: **5[BArF]** Ge1-S1 2.104(7), Ge1-C1 1.990(2), Ge1-C32 2.043(3), Ge1-C25 2.038(3), C1-Ge1-C32 114.60(12), C1-Ge1-C25 106.74(11), C32-Ge1-C25 96.02(11), S1-Ge1-C25 111.23(8), S1-Ge1-C32 108.70(8), S1-Ge1-C1 117.45(8). **6[BArF]** Ge1-Se1 2.237(5), Ge1-C1 1.993(3), Ge1-C32 2.039(4), Ge1-C25 2.039(4), C1-Ge1-C32 114.20(15), C1-Ge1-C25 106.92(14), C32-Ge1-C25 96.17(14), Se1-Ge1-C25 110.27(10), Se1-Ge1-C32 109.14(10), Se1-Ge1-C1 117.90(9).

After examination of the acylium-like nature of compound **3**, we turned our attention towards comparisons to TMO properties. The oxide (O^{2-}) transfer from a terminal TMO to Lewis base was reported.[66-67] Inspired by this we treated compound **3** with a series of Lewis bases, such as PMe_3, PPh_3, IMe_4 and IDipp. However, no reactivity was observed. Treatment of compound **3** with ^{Me}cAAC [1-(2,6-diisopropylphenyl)-3,3,5,5-tetramethylpyrrolidine-2-ylidene), a strong π-acceptor as well as σ-donor], readily afforded compound **2** (yield **2[Cl]** = 92%, **2[BArF]** = 95%) with the concomitant formation of ^{Me}cAAC=O (Scheme 2). DFT calculations on this oxide transfer are also in agreement with the observed experimental findings (Figure S54).

Scheme 3. Reversible activation of CO_2 by 3[Cl] and subsequent hydrosilylation

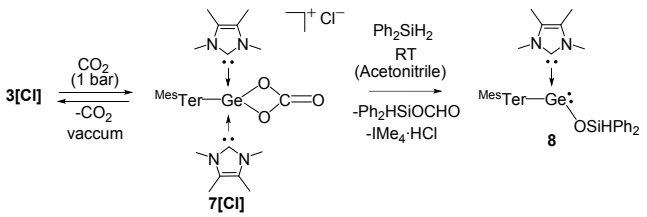

On treating an acetonitrile solution of compound **3** with CO_2 (1 bar) the resulting $^{13}C\{^1H\}$ NMR spectrum revealed a new signal at δ 155.2 ppm, similar to the reported germanium carbonate (δ 154.7 ppm).[21] Additionally, in the ^1H NMR spectrum, a distinct downfield shift was observed for the coordinated NHC

methyl protons (from δ 3.02, δ 3 .03 ppm to δ 3.73 ppm). This points to the formation of a symmetric compound. Surprisingly, these characteristic signals for carbonate species disappear on degassing the solution (Scheme 3). Here, reformation of compound **3** can be observed through comparison of NMR signals (see SI, Figure S23). Such reversibility strongly resembles that of TMOs.[10] However, this reversible binding of CO_2 with Ge-O bond of compound **3** is unprecedented compared to the previously known reactivity of heavier group 14 carbonyls with CO_2.[21-25]

Unfortunately, due to the high instability of the **7** we were unable to confirm its molecular structure by SC-XRD. Addition of 1 eq. of diphenylsilane was carried out under an atmosphere of CO_2, which resulted in formation of the siloxygermylene, compound **8** [^{Mes}TerGe(OSiHPh$_2$)(IMe$_4$)] (Scheme 3). Additionally, a trace amount of silyl formate and IMe$_4$·HCl were observed during this reaction. For compound **8** the carbene carbon was found at δ 157.9 ppm, in the ^{13}C{^{1}H} NMR spectrum, whilst in the ^{29}Si{^{1}H} NMR spectrum the siloxy silicon was observed at δ -22.4 ppm. Furthermore, SC-XRD confirmed the identity of compound **8** (Figure 6), which revealed a tri-coordinate germanium center bonded with one IMe$_4$, siloxy group and ^{Mes}Ter ligand. Expectedly, Ge1-O1 bond length in **8** (1.889(3) Å) is similar to the Ge-O bond length in the NHC-stabilized *tert*-butoxido germylene (1.883(10) Å),[68] but, elongated compared to Ge-O bond length in **3[BArF]** (1.697(3) Å).

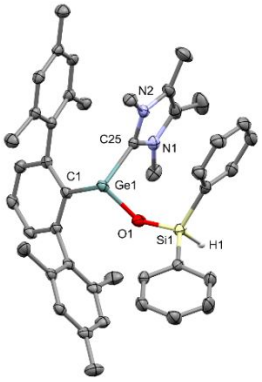

Figure 6. Molecular structures of compound **8** in the solid state. Ellipsoids are set at the 50% probability level; hydrogen atoms (except H1) are omitted for clarity. Selected bond lengths [Å] and bond angles [°]: Ge1-O1 1.889(3), Ge1-C1 2.047(3), Ge1-C25 2.095(3), C1-Ge1-O1 97.06(9), C1-Ge1-C25 97.07(9), O1-Ge1-C25 89.59(9).

Due to the reversible nature of compound **7** and the formation of compound **8**, our interest turned to the catalytic transformation of CO_2, as this indicates the potential for a Ge(II)/(IV) redox based catalytic cycle. We found that compound **3** can transform CO_2 to corresponding hydrosilylated products in both a stoichiometric and catalytic manner in the presence of diphenylsilane (Ph$_2$SiH$_2$). After optimatization, we found use of 2.5 mol% of **3[Cl]**, at 50 °C provides suitable reaction conditions. Complete consumption of Ph$_2$SiH$_2$ is observed within 5 h, by ^{1}H NMR, with the formation of silylformate, bis(silyl)acetal and silylated methanol (Figure S27). Solvent screening found that the reaction best proceeds in polar solvents (e.g. acetonitrile) in comparison to less polar solvents (e.g. benzene). This is attributed to the low solubility of the catalyst in the non-polar solvent. Additionally, to understand the role of the counter anion we have performed this reaction under same conditions with **3[BArF]**. However, no effective change in turnover was observed, concluding that the counter anion does not play an important role in this catalytic cycle. Furthermore, control experiments performed with IMe$_4$, under the optimized reaction conditions, found negligible turnover. Notably, for group 14 metal complexes, there are only a handful examples of catalytic reduction of CO_2.[69-71] One example of heavier group 14 metal complexes was reported by Kato and Baceiredo, which showed hydrosilylation of CO_2 using a *N, P*-heterocyclic germylene and boron FLP-type system (FLP = Frustrated Lewis Pair).[69] Whilst catalytic hydroboration of CO_2 have been successfully demonstrated with N/Si$^+$based FLP system, low valent Ge(II) and Sn(II) hydrides and very recently with the parent silyliumylidene ion.[70-72]

The formation of silylformate during hydrosilylation reactions prompted us to investigate the use of compound **3** in the functionalization of amines. As they have been implicated as key intermediates in the *N*-formylation or *N*-methylation of amines.[8] Accordingly, we have examined the scope of the reductive functionalization of CO_2 with various amines, using Ph$_2$SiH$_2$ as reductant and **3[Cl]** as catalyst (Table 1). The study revealed that aliphatic amines proceed smoothly compared to aromatic amines. This is possibly attributed to the low nucleophilicity of the aromatic amine arising from the delocalization of nitrogen lone pair with the phenyl ring.[73] In general, room temperature catalysis favours formamide formation whereas at elevated temperatures *N*-methylation is the major product along with reduced reaction times, which is in line with a recent study reported by Nguyen and co-workers.[74] In the cases of morpholine and *N*-methylaniline subsequent formation of formamide, aminal and methylated amine are observed as mixture, which are the 2e-, 4e- and 6e-reduced products of CO_2 (Table 1). Again control reactions with IMe$_4$ and IMe$_4$.HCl under the standard reaction conditions revealed negligible turnover.

Table 1. N-Methylation of amines using 1 bar CO_2, 3 eq. Ph$_2$SiH$_2$, in CD$_3$CN and 2.5 mol% of 3[Cl].

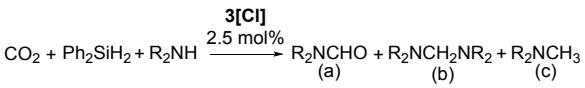

Amine	Temp (° C)	Time (h)	NMR Yield[a]		
			a	b	c
Diethylamine	20	6	28	-	70
	50	2	15	-	82
Piperidine	20	12	27	-	72
	50	2	18	-	80
Morpholine	20	10	22	32	35
	50	3	21	-	75
Dicyclohexylamine	20	5	57	-	42
	50	3	16	-	78

N-Methylaniline	20	24	41	10	38
	50	15	16	5	85

*For all amines 99% conversion was observed. NMR yields were calculated according to the NMR standard (trimethoxy benzene).

A series of stoichiometric reactions were undertaken to probe the mechanism. Compound **3** was found to be inert towards amine, whilst it reacts with CO_2 (*vide supra*) and Ph_2SiH_2.

Scheme 4. Proposed mechanism for the germanium catalysed *N*-functionalization of amine with CO_2. ΔG_L^S (kcal mol^{-1}) values are given in brackets.

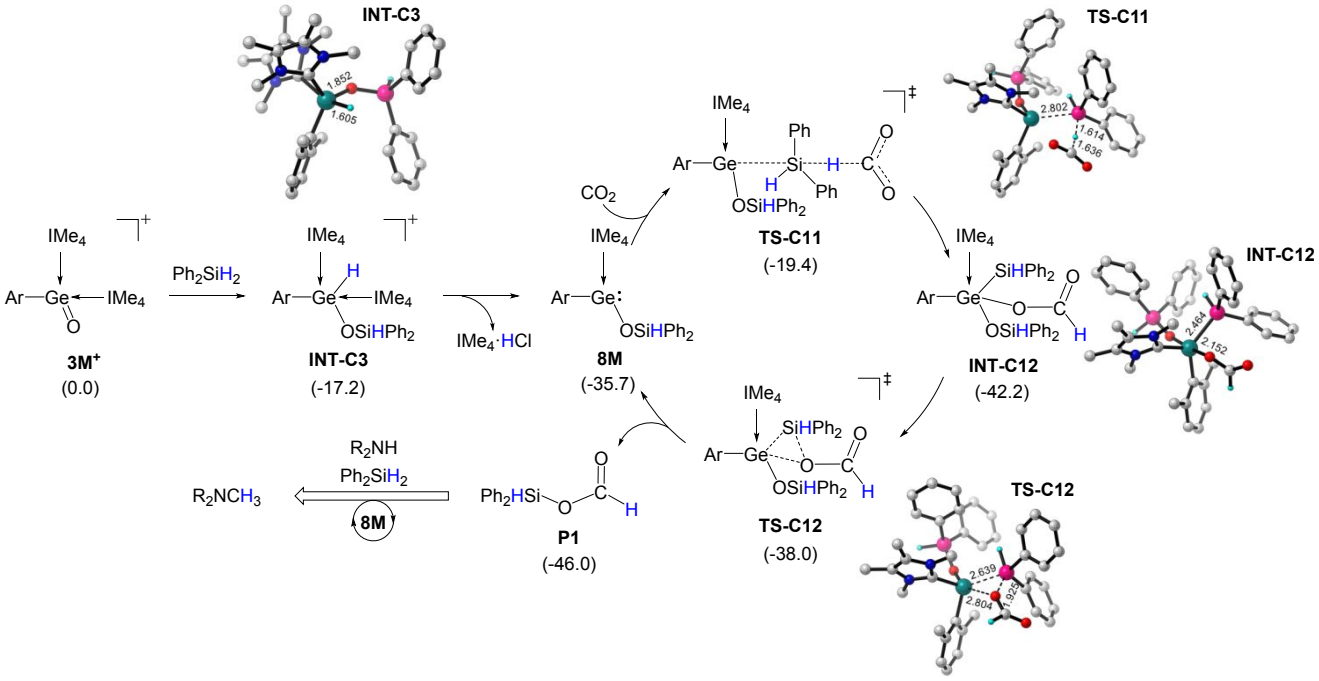

Suggesting either initial coordination of CO_2 or silane to compound **3**. Interestingly, stoichiometric reaction of **3** with Ph_2SiH_2, in the absence of CO_2, afforded the siloxygermylene **8** quantitatively (yield = 80%), with the concomitant formation of imidazolium chloride. Futhermore, we found that compound **8** is able to transform CO_2 to the corresponding *N*-functionalized products in both a stoichiometric and catalytic manner. Use of 2.5 mol% of **8** in the reductive funcationalization of morpholine, under the standard reactions conditions, led to similar results to that observed with compound **3** at both temperatures (see SI, Figure S48-49). This suggests that **8** may infact be the resting state of the active cycle. However, stoichiometric reactions of **8** with the induvial components resulted in no reaction, therefore suggesting a cooperative effect between the reaction components is required for turnover to be achieved.

Based on experimental data there are two potential pathways for entry into the active catalytic cycle: (i) coordination of CO_2 to form carbonate (akin to Compound **7**) and subsequent reduction by silane or (ii) initial silane reduction then CO_2 activation. We, therefore, have performed DFT calculations to unveil the mechanistic underpinnings of the germanium mediated catalytic reactions. These were performed using reduced models, with the ^{Mes}Ter ligand replaced with 2,6-dimethylphenyl (Ar). Firstly, pathway (i) was examined and found the binding of CO_2 to the Ge–O^1 bond in **3M$^+$** leads to the formation of slightly stable germanium carbonate (**INT-C1**), by overcoming a very low energy barrier of only 1.0 kcal mol^{-1} (Figures S55). However, the reduction of **INT-C1** by silane to produce formoxysilane (**P1**) demands extremely high energy barrier of 35.7 kcal mol^{-1}. Hence, theoretical calculations suggest that pathway (i) is unfavorable.

Alternative pathway (ii), where **3M$^+$** is initially reduced by Ph_2SiH_2, requires an energy barrier of 2.1 kcal mol^{-1} to afford the significantly more stable Ge(IV)-hydride species (**INT-C3**). From here, dissociation of IMe_4 followed by CO_2 coordination/insertion into the Ge(IV)-hydride was found to be unfavourable with a high energy barrier of 45.4 kcal mol^{-1} (Figure S56). On the other hand, keeping IMe_4 within the vicinity of Ge(IV) enables the Lewis base to abstract the proton

from the Ge center with a very low activation barrier of 0.4 kcal mol^{-1}). The resulting intermediate finally delivers the siloxygermylene (**8M**) and IMe_4·HCl is also formed with the assistance of the chloride counter anion (Scheme 4).

The role of **8M** in the formation of formoxysilane (**P1**) was explored (Scheme 4). This is proposed to occur in a concerted process via **TS-C11**, in which the free CO_2 acts as a hydride acceptor from the hypercoordinate silane (Figure S58). The resulting intermediate **INT-C12** finally delivers formoxysilane accompanying an energy barrier of 4.2 kcal mol^{-1}. Alternate pathways, where the CO_2 first coordinates to **8M** followed by reduction or via oxidative addition of Si-H across the Ge(II) centre were also explored, demanding the energy barriers of 20.5 and 16.7 kcal mol^{-1}, respectively (Figure S59). Therefore the second alternate route exhibiting slightly higher energy barrier compared to that for the concerted process depicted in Scheme 4, may be operative independently under the reaction conditions. To further validate the proposed mechanism, selected transition states were calculated using the full m-terphenyl ligand (**8**), rather than the truncated model system (**8M**). These show comparable energy barriers (Table S1) and thus support the proposed mechanism as highlighted in Scheme 4.

The Ge(II) siloxygermylene species (**8**) is therefore proposed as the active catalyst in the generation of formoxysilane, which is key for further functionalization with amines. Compound **8** is accessible from the reaction of the germaacylium ion precatalyst (**3**) and silane. Notably, this is different to other reported heavier carbonyl hydrosilylation reactions. Here we have shown the retention of the low valent Ge(II) centre, whereas previous hydrosilylation of E=O (E = Si, Ge) bonds results in the formation of the higher oxidation state oxo-silyl species.[21-23, 31]

CONCLUSION

In summary, we have shown the successful isolation of a donor-stablised germaacylium ion (**3**). Analogous to classical acylium ions, this provides access to novel germanium analogs of carbonyl and heavier chalcogen derivatives, exemplified by the first example of a NHC-supported germanium ester. Moreover, its transition metal oxide like-behaviour was investigated, where the regeneration of germyliumylidene (**2**) was achieved via oxide transfer to ^{Me}cAAC representing diverse electronic features of this heavier acylium analog. This TMO behavour was further exploited in CO_2 functionalization reactions, where reversible CO_2 coordination was observed as well as the ability of **3** to act as a pre-catalyst in CO_2 hydrosilylation and N-methylation of amines. A combined theoretical and experimental approach revealed a Ge(II) siloxygermylene species (**8**) to be the active species. This report further demonstrates the ability of main group metals to mimic their transition metal counterparts, whilst also showing similar reactivity to that of the lightest group 14 congener.

ASSOCIATED CONTENT

Supporting Information

The Supporting Information is available free of charge on the ACS Publications website at DOI:

Crystallographic data (CCDC 2006663-2006668), experimental procedures, full spectroscopic analysis, and DFT calculations.

AUTHOR INFORMATION

Corresponding Author

*E-Mail for S.I.: s.inoue@tum.de

D.K.: koley@iiserkol.ac.in

Notes

The authors declare no competing financial interests.

ACKNOWLEDGMENT

We gratefully acknowledge financial support from WACKER Chemie AG, the European Research Council (SILION 637394) andthe DAAD (fellowship for D.S.). This project has received funding from the European Union's Horizon 2020 research and innovation program under the Marie Skłodowska-Curie grant agreement No 754462 (Fellowship CW). S. D. acknowledges the CSIR, India for the Senior Research Fellowship (SRF) and IISER Kolkata for the computational facility. D. K. acknowledges the funding from bilateral DST-DFG (INT/FRG/DFG/P-05/2017) scheme.

REFERENCES

1. Liu, Q.; Wu, L.; Jackstell, R.; Beller, M., Using carbon dioxide as a building block in organic synthesis. *Nat. Commun.* **2015,** *6* (1), 5933.

2. Maeda, C.; Miyazaki, Y.; Ema, T., Recent progress in catalytic conversions of carbon dioxide. *Catal. Sci. Technol.* **2014,** *4* (6), 1482-1497.

3. Fernández-Alvarez, F. J.; Oro, L. A., Homogeneous Catalytic Reduction of CO_2 with Silicon-Hydrides, State of the Art. *ChemCatChem* **2018,** *10* (21), 4783-4796.

4. Chen, J.; McGraw, M.; Chen, E. Y.-X., Diverse Catalytic Systems and Mechanistic Pathways for Hydrosilylative Reduction of CO_2. *ChemSusChem* **2019,** *12* (20), 4543-4569.

5. Wang, X.; Xia, C.; Wu, L., Homogeneous carbon dioxide reduction with p-block element-containing reductants. *Green Chem.* **2018,** *20* (24), 5415-5426.

6. Zhang, Y.; Zhang, T.; Das, S., Catalytic transformation of CO_2 into C1 chemicals using hydrosilanes as a reducing agent. *Green Chem.* **2020,** *22*, 1800-1820.

7. Fernández-Alvarez, F. J.; Aitani, A. M.; Oro, L. A., Homogeneous catalytic reduction of CO_2 with hydrosilanes. *Catal. Sci. Technol.* **2014,** *4* (3), 611-624.

8. Das Neves Gomes, C.; Jacquet, O.; Villiers, C.; Thuéry, P.; Ephritikhine, M.; Cantat, T., A Diagonal Approach to Chemical Recycling of Carbon Dioxide: Organocatalytic Transformation for the Reductive Functionalization of CO_2. *Angew. Chem. Int. Ed.* **2012,** *51* (1), 187-190.

9. Silvia, J. S.; Cummins, C. C., Binding, release, and functionalization of CO_2 at a nucleophilic oxo anion complex of titanium. *Chem. Sci.* **2011,** *2* (8), 1474-1479.

10. Knopf, I.; Ono, T.; Temprado, M.; Tofan, D.; Cummins, C. C., Uptake of one and two molecules of CO_2 by the molybdate dianion: a soluble, molecular oxide model system for carbon dioxide fixation. *Chem. Sci.* **2014,** *5* (5), 1772-1776.

11. Paparo, A.; Silvia, J. S.; Spaniol, T. P.; Okuda, J.; Cummins, C. C., Countercation Effect on CO2 Binding to Oxo Titanate with Bulky Anilide Ligands. *Chem. Eur. J.* **2018,** *24* (64), 17072-17079.

12. Kamata, K.; Sugahara, K., Base Catalysis by Mono- and Polyoxometalates. *Catalysts* **2017,** *7* (11), 345.

13. Morris, D. S.; Weetman, C.; Wennmacher, J. T. C.; Cokoja, M.; Drees, M.; Kühn, F. E.; Love, J. B., Reduction of carbon dioxide and organic carbonyls by hydrosilanes catalysed by the perrhenate anion. *Catal. Sci. Technol.* **2017,** *7* (13), 2838-2845.

14. Wang, M.-Y.; Wang, N.; Liu, X.-F.; Qiao, C.; He, L.-N., Tungstate catalysis: pressure-switched 2- and 6-electron reductive functionalization of CO_2 with amines and phenylsilane. *Green Chem.* **2018,** *20* (7), 1564-1570.

15. Mazzotta, M. G.; Xiong, M.; Abu-Omar, M. M., Carbon Dioxide Reduction to Silyl-Protected Methanol Catalyzed by an Oxorhenium Pincer PNN Complex. *Organometallics.* **2017,** *36* (9), 1688-1691.

16. Power, P. P., Main-group elements as transition metals. *Nature* **2010,** *463* (7278), 171-177.

17. Weetman, C.; Inoue, S., The Road Travelled: After Main-Group Elements as Transition Metals. *ChemCatChem* **2018,** *10* (19), 4213-4228.

18. Hadlington, T. J.; Driess, M.; Jones, C., Low-valent group 14 element hydride chemistry: towards catalysis. *Chem. Soc. Rev.* **2018,** *47* (11), 4176-4197.

19. Stephan, D. W., Frustrated Lewis Pairs. *J. Am. Chem. Soc.* **2015,** *137* (32), 10018-10032.

20. Xiong, Y.; Yao, S.; Driess, M., Chemical Tricks To Stabilize Silanones and Their Heavier Homologues with E=O Bonds (E=Si–Pb): From Elusive Species to Isolable Building Blocks. *Angew. Chem. Int. Ed.* **2013,** *52* (16), 4302-4311.

21. Li, L.; Fukawa, T.; Matsuo, T.; Hashizume, D.; Fueno, H.; Tanaka, K.; Tamao, K., A stable germanone as the first isolated heavy ketone with a terminal oxygen atom. *Nat. Chem.* **2012,** *4*, 361.

22. Alvarado-Beltran, I.; Rosas-Sánchez, A.; Baceiredo, A.; Saffon-Merceron, N.; Branchadell, V.; Kato, T., A Fairly Stable Crystalline Silanone. *Angew. Chem. Int. Ed.* **2017,** *56* (35), 10481-10485.

23. Rosas-Sánchez, A.; Alvarado-Beltran, I.; Baceiredo, A.; Saffon-Merceron, N.; Massou, S.; Hashizume, D.; Branchadell, V.; Kato, T., Cyclic (Amino)(Phosphonium Bora-Ylide)Silanone: A Remarkable Room-Temperature-Persistent Silanone. *Angew. Chem. Int. Ed.* **2017,** *56* (50), 15916-15920.

24. Wendel, D.; Reiter, D.; Porzelt, A.; Altmann, P. J.; Inoue, S.; Rieger, B., Silicon and Oxygen's Bond of Affection: An Acyclic Three-Coordinate Silanone and Its Transformation to an Iminosiloxysilylene. *J. Am. Chem. Soc.* **2017,** *139* (47), 17193-17198.

25. Burchert, A.; Yao, S.; Müller, R.; Schattenberg, C.; Xiong, Y.; Kaupp, M.; Driess, M., An Isolable Silicon Dicarbonate Complex from Carbon Dioxide Activation with a Silylone. *Angew. Chem. Int. Ed.* **2017,** *56* (7), 1894-1897.

26. Rodriguez, R.; Alvarado-Beltran, I.; Saouli, J.; Saffon-Merceron, N.; Baceiredo, A.; Branchadell, V.; Kato, T., Reversible CO_2 Addition to a Si=O Bond and Synthesis of a Persistent SiO_2–CO_2 Cycloadduct Stabilized by a Lewis Donor–Acceptor Ligand. *Angew. Chem. Int. Ed.* **2018,** *57* (10), 2635-2638.

27. Anker, M. D.; Coles, M. P., Aluminium-Mediated Carbon Dioxide Reduction by an Isolated Monoalumoxane Anion. *Angew. Chem. Int. Ed.* **2019,** *58* (50), 18261-18265.

28. Hicks, J.; Heilmann, A.; Vasko, P.; Goicoechea, J. M.; Aldridge, S., Trapping and Reactivity of a Molecular Aluminium Oxide Ion. *Angew. Chem. Int. Ed.* **2019,** *58* (48), 17265-17268.

29. Weetman, C.; Bag, P.; Szilvási, T.; Jandl, C.; Inoue, S., CO2 Fixation and Catalytic Reduction by a Neutral Aluminum Double Bond. *Angew. Chem. Int. Ed.* **2019,** *58* (32), 10961-10965.

30. Xiong, Y.; Yao, S.; Müller, R.; Kaupp, M.; Driess, M., Activation of Ammonia by a Si═O Double Bond and Formation of a Unique Pair of Sila-Hemiaminal and Silanoic Amide Tautomers. *J. Am. Chem. Soc.* **2010,** *132* (20), 6912-6913.

31. Kobayashi, R.; Ishida, S.; Iwamoto, T., An Isolable Silicon Analogue of a Ketone that Contains an Unperturbed Si=O Double Bond. *Angew. Chem. Int. Ed.* **2019,** *58* (28), 9425-9428.

32. Spikes, G. H.; Peng, Y.; Fettinger, J. C.; Steiner, J.; Power, P. P., Different reactivity of the heavier group 14 element alkyne analogues Ar′MMAr′ (M = Ge, Sn; Ar′ = C_6H_3-2,6(C_6H_3-2,6-Pri_2)$_2$) with R_2NO. *Chem. Commun.* **2005,** (48), 6041-6043.

33. Wang, X.; Zhu, Z.; Peng, Y.; Lei, H.; Fettinger, J. C.; Power, P. P., Room-Temperature Reaction of Carbon Monoxide with a Stable Diarylgermylene. *J. Am. Chem. Soc.* **2009,** *131* (20), 6912-6913.

34. Del Rio, N.; Baceiredo, A.; Saffon-Merceron, N.; Hashizume, D.; Lutters, D.; Müller, T.; Kato, T., A Stable Heterocyclic Amino(phosphanylidene-σ4-phosphorane) Germylene. *Angew. Chem. Int. Ed.* **2016,** *55* (15), 4753-4758.

35. Fukuda, T.; Hashimoto, H.; Sakaki, S.; Tobita, H., Stabilization of a Silaaldehyde by its η2 Coordination to Tungsten. *Angew. Chem. Int. Ed.* **2016,** *55* (1), 188-192.

36. Dube, J. W.; Graham, C. M. E.; Macdonald, C. L. B.; Brown, Z. D.; Power, P. P.; Ragogna, P. J., Reversible, Photoinduced Activation of P_4 by Low-Coordinate Main Group Compounds. *Chem. Eur. J.* **2014,** *20* (22), 6739-6744.

37. Usher, M.; Protchenko, A. V.; Rit, A.; Campos, J.; Kolychev, E. L.; Tirfoin, R.; Aldridge, S., A Systematic Study of Structure and E–H Bond Activation Chemistry by Sterically Encumbered Germylene Complexes. *Chem. Eur. J.* **2016,** *22* (33), 11685-11698.

38. Del Rio, N.; Lopez-Reyes, M.; Baceiredo, A.; Saffon-Merceron, N.; Lutters, D.; Müller, T.; Kato, T., N,P-Heterocyclic Germylene/$B(C_6F_5)_3$ Adducts: A Lewis Pair with Multi-reactive Sites. *Angew. Chem. Int. Ed.* **2017,** *56* (5), 1365-1370.

39. Schneider, J.; Sindlinger, C. P.; Freitag, S. M.; Schubert, H.; Wesemann, L., Diverse Activation Modes in the Hydroboration of Aldehydes and Ketones with Germanium, Tin, and Lead Lewis Pairs. *Angew. Chem. Int. Ed.* **2017,** *56* (1), 333-337.

40. Sugahara, T.; Guo, J.-D.; Sasamori, T.; Nagase, S.; Tokitoh, N., Regioselective Cyclotrimerization of Terminal Alkynes Using a Digermyne. *Angew. Chem. Int. Ed.* **2018,** *57* (13), 3499-3503.

41. Swamy, V. S. V. S. N.; Pal, S.; Khan, S.; Sen, S. S., Cations and dications of heavier group 14 elements in low oxidation states. *Dalton Trans.* **2015,** *44* (29), 12903-12923.

42. Engesser, T. A.; Lichtenthaler, M. R.; Schleep, M.; Krossing, I., Reactive p-block cations stabilized by weakly coordinating anions. *Chem. Soc. Rev.* **2016,** *45* (4), 789-899.

43. Benzi, P.; Operti, L.; Vagilo, A.G.; Splendore, M.; Volpe, P.; Speranca, M.; Gabrielli, R., Gas phase ion-molecule reactions of monogermane with oxygen and ammonia. *J. Organomet. Chem.* **1988,** *354* (1), 39-50.

44. Rit, A.; Tirfoin, R.; Aldridge, S., Exploiting Electrostatics To Generate Unsaturation: Oxidative Ge=E Bond Formation Using a Non π-Donor Stabilized [R(L)Ge:]+ Cation. *Angew. Chem. Int. Ed.* **2016,** *55* (1), 378-382.

45. Xiong, Y.; Szilvási, T.; Yao, S.; Tan, G.; Driess, M., Synthesis and Unexpected Reactivity of Germyliumylidene Hydride [:GeH]+ Stabilized by a Bis(N-heterocyclic carbene)borate Ligand. *J. Am. Chem. Soc.* **2014,** *136* (32), 11300-11303.

46. Xiong, Y.; Yao, S.; Inoue, S.; Berkefeld, A.; Driess, M., Taming the germyliumylidene [CIGe:]+ and germathionium [CIGe=S]+ ions by donor–acceptor stabilization using 1,8-bis(tributylphosphazenyl)naphthalene. *Chem. Commun.* **2012,** *48* (100), 12198-12200.

47. Roy, M. M. D.; Fujimori, S.; Ferguson, M. J.; McDonald, R.; Tokitoh, N.; Rivard, E., Neutral, Cationic and Hydride-substituted Siloxygermylenes. *Chem. Eur. J.* **2018,** *24* (54), 14392-14399.

48. Xiong, Y.; Yao, S.; Tan, G.; Inoue, S.; Driess, M., A Cyclic Germadicarbene ("Germylone") from Germyliumylidene. *J. Am. Chem. Soc.* **2013,** *135* (13), 5004-5007.

49. Yao, S.; Xiong, Y.; Driess, M., From NHC→germylenes to stable NHC→germanone complexes. *Chem. Commun.* **2009,** (42), 6466-6468.

50. Yao, S.; Xiong, Y.; Wang, W.; Driess, M., Synthesis, Structure, and Reactivity of a Pyridine-Stabilized Germanone. *Chem. Eur. J.* **2011,** *17* (17), 4890-4895.

51. Rupar, P. A.; Staroverov, V. N.; Baines, K. M., Reactivity Studies of N-Heterocyclic Carbene Complexes of Germanium(II). *Organometallics.* **2010,** *29* (21), 4871-4881.

52. Sharma, M. K.; Sinhababu, S.; Mahawar, P.; Mukherjee, G.; Pandey, B.; Rajaraman, G.; Nagendran, S., Donor–acceptor-stabilised germanium analogues of acid chloride, ester, and acyl pyrrole compounds: synthesis and reactivity. *Chem. Sci.* **2019,** *10* (16), 4402-4411.

53. Sinhababu, S.; Yadav, D.; Karwasara, S.; Sharma, M. K.; Mukherjee, G.; Rajaraman, G.; Nagendran, S., The Preparation of Complexes of Germanone from a Germanium μ-Oxo Dimer. *Angew. Chem. Int. Ed.* **2016,** *55* (27), 7742-7746.

54. Bakthavachalam, K.; Yuvaraj, K.; Mondal, B.; Prakash, R.; Ghosh, S., All-metallagermoxane with an adamantanoid cage structure: $[(Cp^*Ru(CO)_2Ge)_4(\mu\text{-}O)_6]$ (Cp^* = $\eta5\text{-}C_5Me_5$). *Dalton Trans.* **2015,** *44* (41), 17920-17923.

55. Reiter, D.; Frisch, P.; Szilvási, T.; Inoue, S., Heavier Carbonyl Olefination: The Sila-Wittig Reaction. *J. Am. Chem. Soc.* **2019,** *141* (42), 16991-16996.

56. Ozturk, T.; Ertas, E.; Mert, O., Use of Lawesson's Reagent in Organic Syntheses. *Chem. Rev.* **2007,** *107* (11), 5210-5278.

57. Hua, G.; Woollins, J. D., Formation and Reactivity of Phosphorus–Selenium Rings. *Angew. Chem. Int. Ed.* **2009,** *48* (8), 1368-1377.

58. Byrne, P. A.; Gilheany, D. G., The modern interpretation of the Wittig reaction mechanism. *Chem. Soc. Rev.* **2013,** *42* (16), 6670-6696.

59. Veith, M.; Becker, S.; Huch, V., A Base-Stabilized Ge–S Double Bond. *Angew. Chem. Int. Ed.* **1989,** *28* (9), 1237-1238.

60. Siwatch, R. K.; Karwasara, S.; Sharma, M. K.; Mondal, S.; Mukherjee, G.; Rajaraman, G.; Nagendran, S., Reactivity of LGe–NR2 and LGe(E)–NR_2 over LGe–Cl and LGe(E)–Cl toward Me3SiX (L = Aminotroponiminate; NR_2 = $N(SiMe_3)_2/NC_4H_4$; E = S/Se; X = Br/CN). *Organometallics.* **2016,** *35* (4), 429-438.

61. Harris, L. M.; Tam, E. C. Y.; Cummins, S. J. W.; Coles, M. P.; Fulton, J. R., The Reactivity of Germanium Phosphanides with Chalcogens. *Inorg. Chem.* **2017,** *56* (5), 3087-3094.

62. Pineda, L. W.; Jancik, V.; Roesky, H. W.; Herbst-Irmer, R., Germacarboxylic Acid: An Organic-Acid Analogue Based on a Heavier Group 14 Element. *Angew. Chem. Int. Ed.* **2004,** *43* (41), 5534-5536.

63. Ossig, G.; Meller, A.; Brönneke, C.; Müller, O.; Schäfer, M.; Herbst-Irmer, R., Bis[(2-pyridyl)bis(trimethylsilyl)methyl-C,N]germanium(II): A Base-Stabilized Germylene and the Corresponding Germanethione, Germaneselenone, and Germanetellurone. *Organometallics* **1997,** *16* (10), 2116-2120.

64. Xiong, Y.; Yao, S.; Karni, M.; Kostenko, A.; Burchert, A.; Apeloig, Y.; Driess, M., Heavier congeners of CO and CO_2 as ligands: from zero-valent germanium ('germylone') to isolable monomeric GeX and GeX2 complexes (X = S, Se, Te). *Chem. Sci.* **2016,** *7* (8), 5462-5469.

65. Matsumoto, T.; Tokitoh, N.; Okazaki, R., The First Kinetically Stabilized Germanethiones and Germaneselones: Syntheses, Structures, and Reactivities. *J. Am. Chem. Soc.* **1999,** *121* (38), 8811-8824.

66. Smeltz, J. L.; Lilly, C. P.; Boyle, P. D.; Ison, E. A., The Electronic Nature of Terminal Oxo Ligands in Transition-Metal Complexes: Ambiphilic Reactivity of Oxorhenium Species. *J. Am. Chem. Soc.* **2013,** *135* (25), 9433-9441.

67. Lohrey, T. D.; Bergman, R. G.; Arnold, J., Reductions of a Rhenium(III) Terminal Oxo Complex by Isocyanides and Carbon Monoxide. *Organometallics* **2018,** *37* (20), 3552-3557.

68. Paul, D.; Heins, F.; Krupski, S.; Hepp, A.; Daniliuc, C. G.; Klahr, K.; Neugebauer, J.; Glorius, F.; Hahn, F. E., Synthesis and Reactivity of Intramolecularly NHC-Stabilized Germylenes and Stannylenes. *Organometallics* **2017,** *36* (5), 1001-1008.

69. Del Rio, N.; Lopez-Reyes, M.; Baceiredo, A.; Saffon-Merceron, N.; Lutters, D.; Müller, T.; Kato, T., N,P-Heterocyclic Germylene/$B(C_6F_5)_3$ Adducts: A Lewis Pair with Multi-reactive Sites. *Angew. Chem. Int. Ed.* **2017,** *56* (5), 1365-1370.

70. Hadlington, T. J.; Kefalidis, C. E.; Maron, L.; Jones, C., Efficient Reduction of Carbon Dioxide to Methanol Equivalents Catalyzed by Two-Coordinate Amido–Germanium(II) and –Tin(II) Hydride Complexes. *ACS Catalysis* **2017,** *7* (3), 1853-1859.

71. Leong, B.-X.; Lee, J.; Li, Y.; Yang, M.-C.; Siu, C.-K.; Su, M.-D.; So, C.-W., A Versatile NHC-Parent Silyliumylidene Cation for Catalytic Chemo- and Regioselective Hydroboration. *J. Am. Chem. Soc.* **2019,** *141* (44), 17629-17636.

72. von Wolff, N.; Lefèvre, G.; Berthet, J. C.; Thuéry, P.; Cantat, T., Implications of CO2 Activation by Frustrated Lewis Pairs in the Catalytic Hydroboration of CO2: A View Using N/Si+ Frustrated Lewis Pairs. *ACS Catal.* **2016,** *6* (7), 4526-4535.

73. Henderson, W. A.; Schultz, C. J., The Nucleophilicity of Amines. *J. Org. Chem.* **1962,** *27* (12), 4643-4646.

74. Nicholls, R. L.; McManus, J. A.; Rayner, C. M.; Morales-Serna, J. A.; White, A. J. P.; Nguyen, B. N., Guanidine-Catalyzed Reductive Amination of Carbon Dioxide with Silanes: Switching between Pathways and Suppressing Catalyst Deactivation. *ACS Catal.* **2018,** *8* (4), 3678-3687.

Insert Table of Contents artwork here

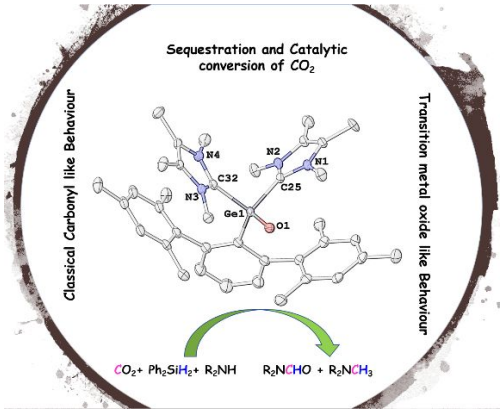

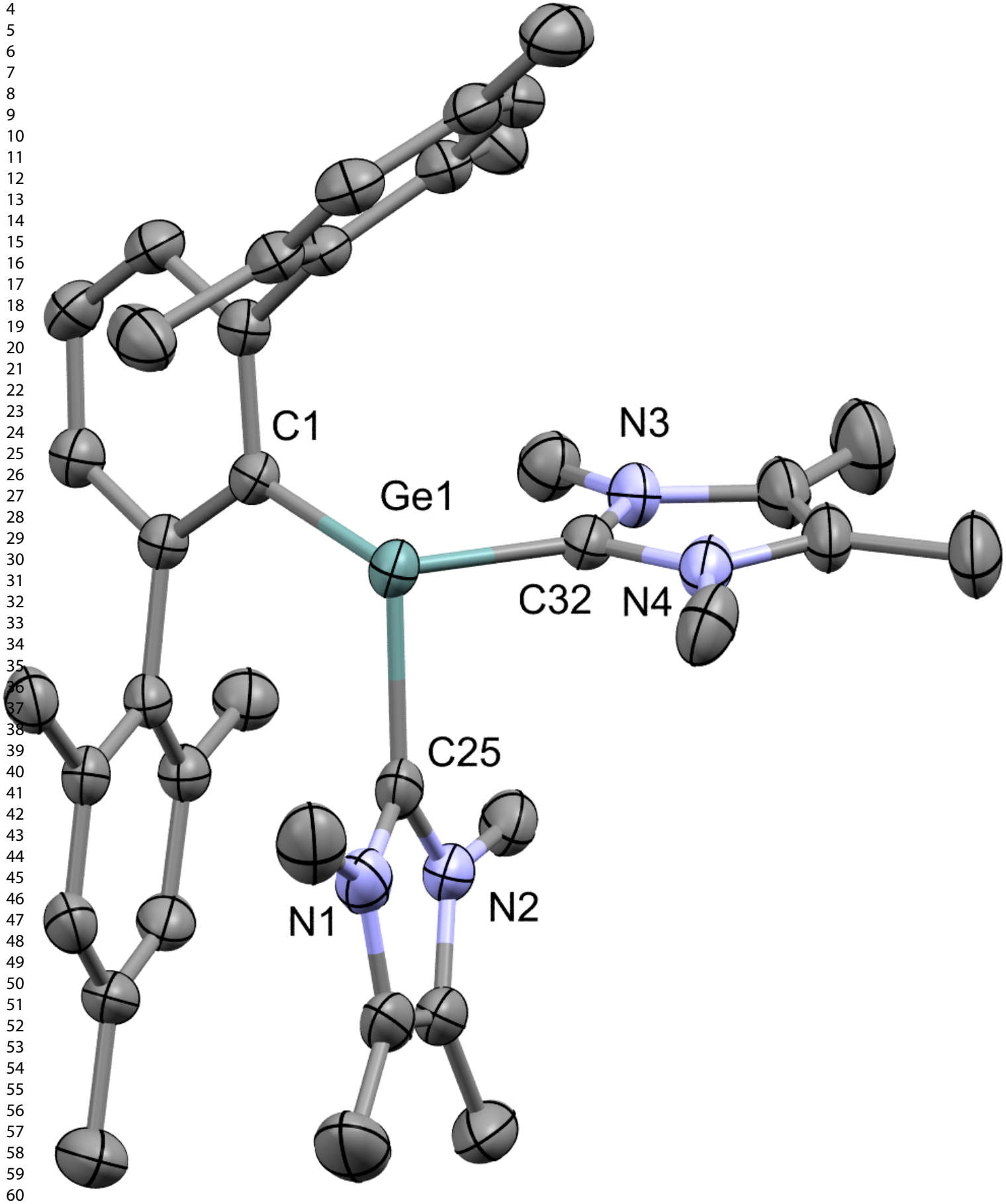
C1
N3
Ge1
C32
N4
C25
N1
N2

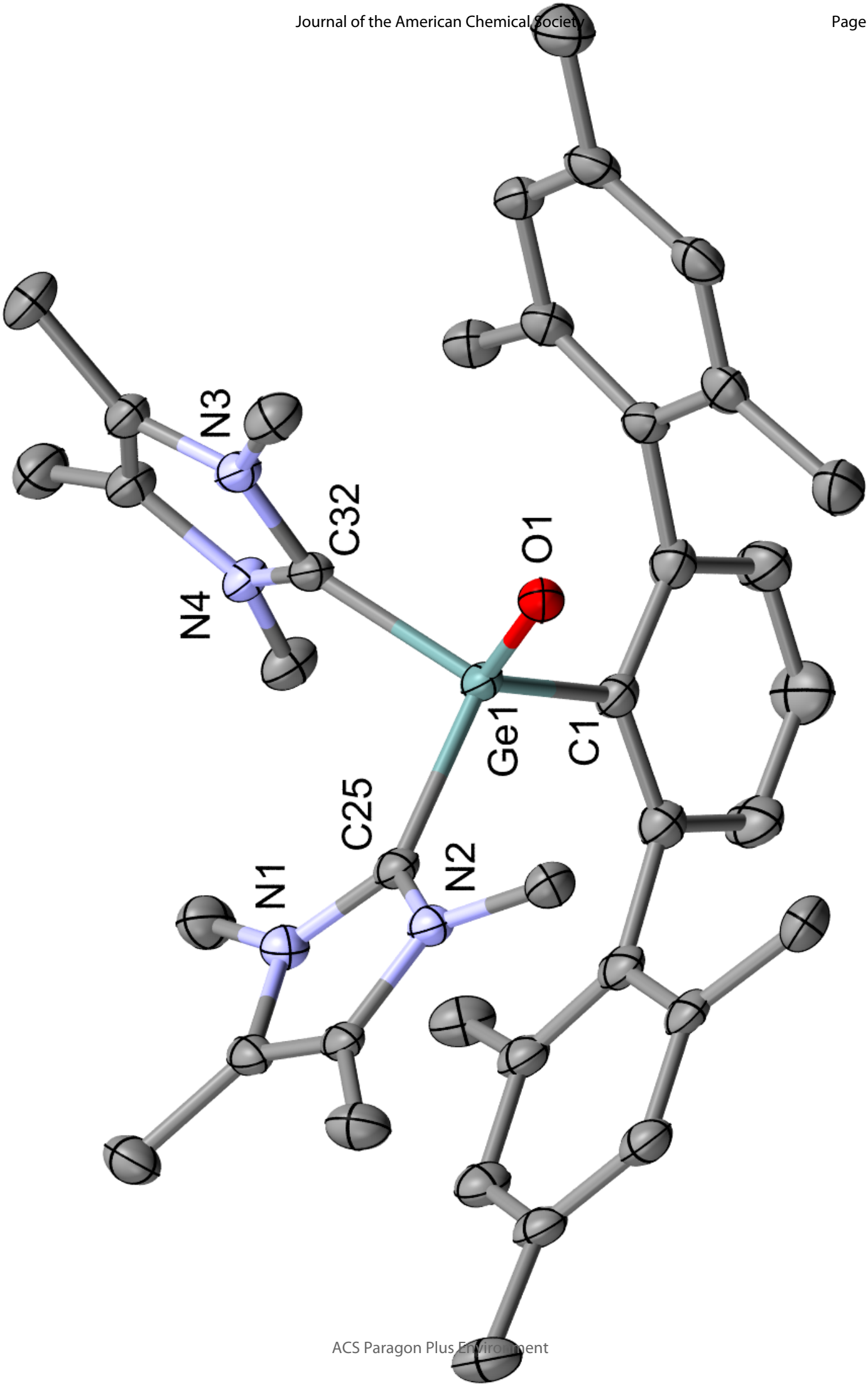
N3
C32
O1
N4
Ge1
C1
C25
N2
N1

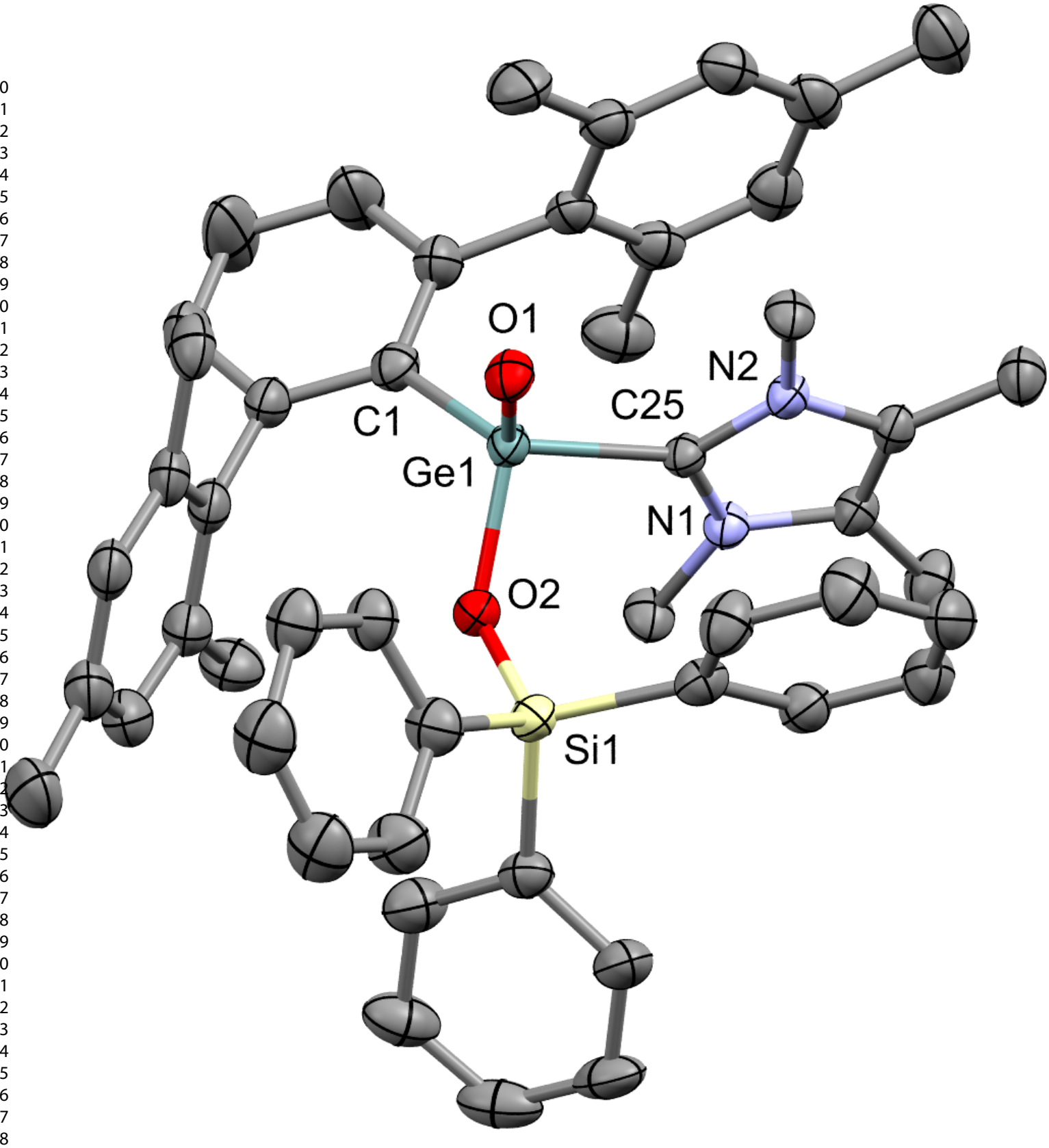
O1
N2
C1
C25
Ge1
N1
O2
Si1

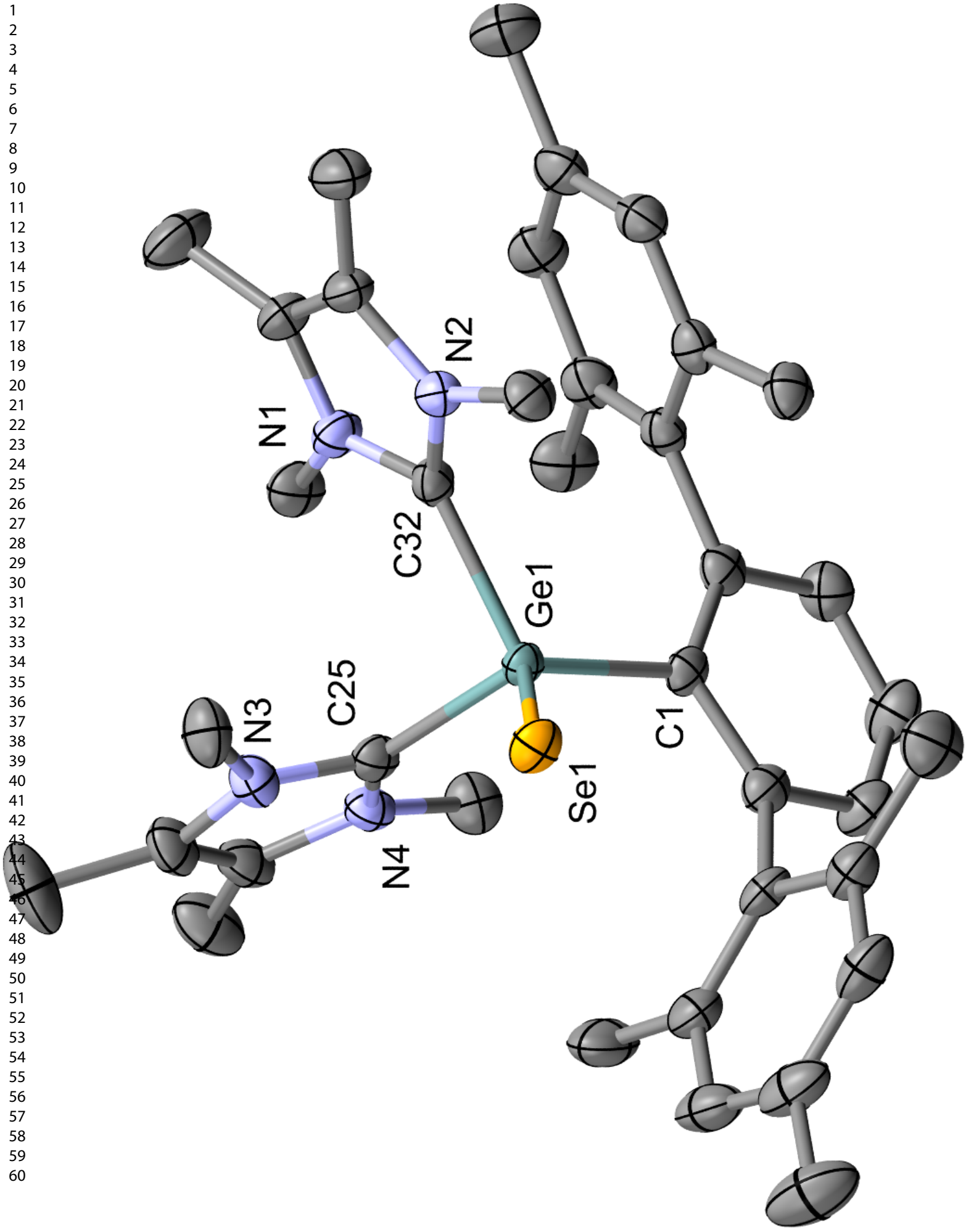
N2
N1
C32
Ge1
C25
N3
C1
Se1
N4

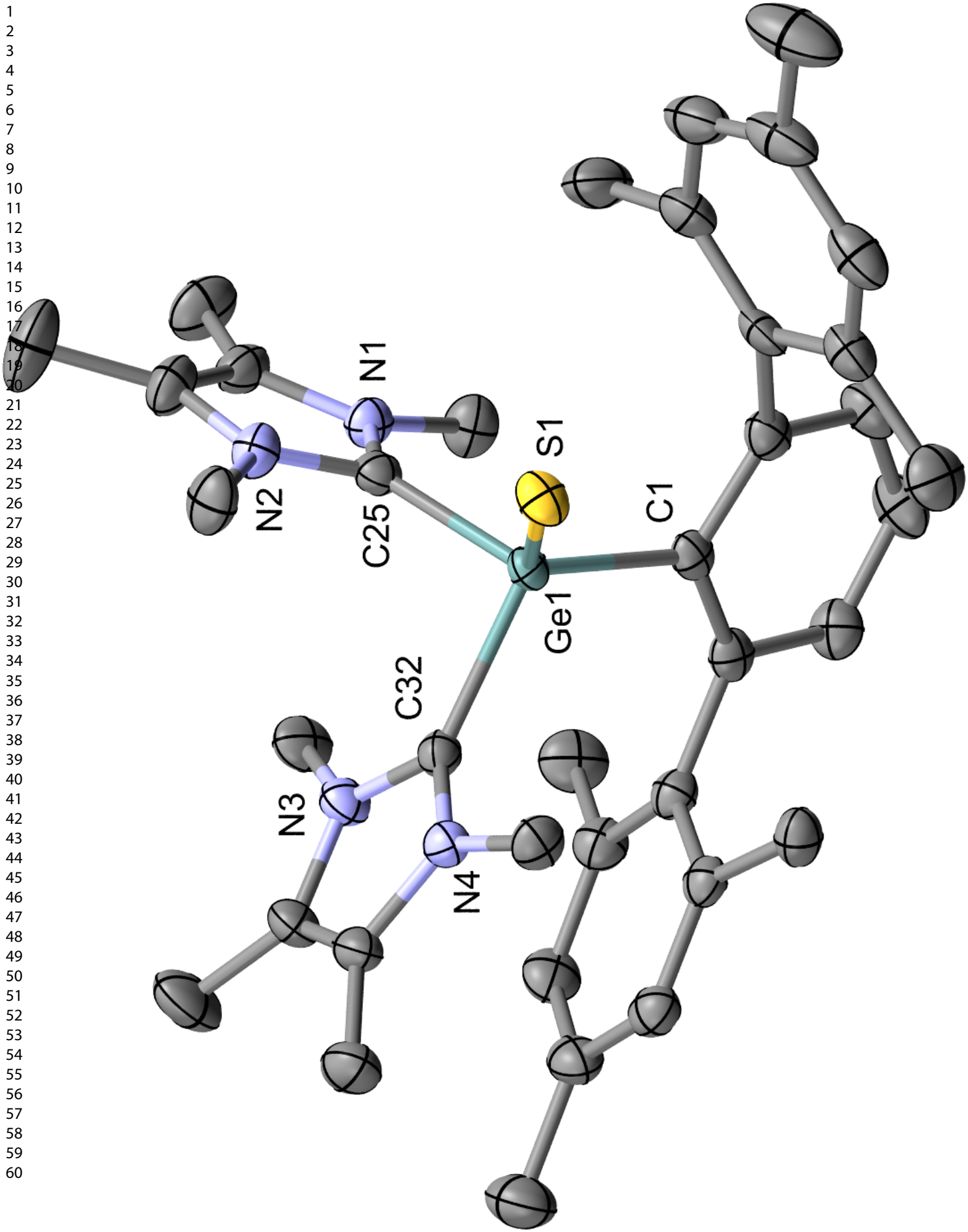
N1
S1
N2
C25
C1
Ge1
C32
N3
N4

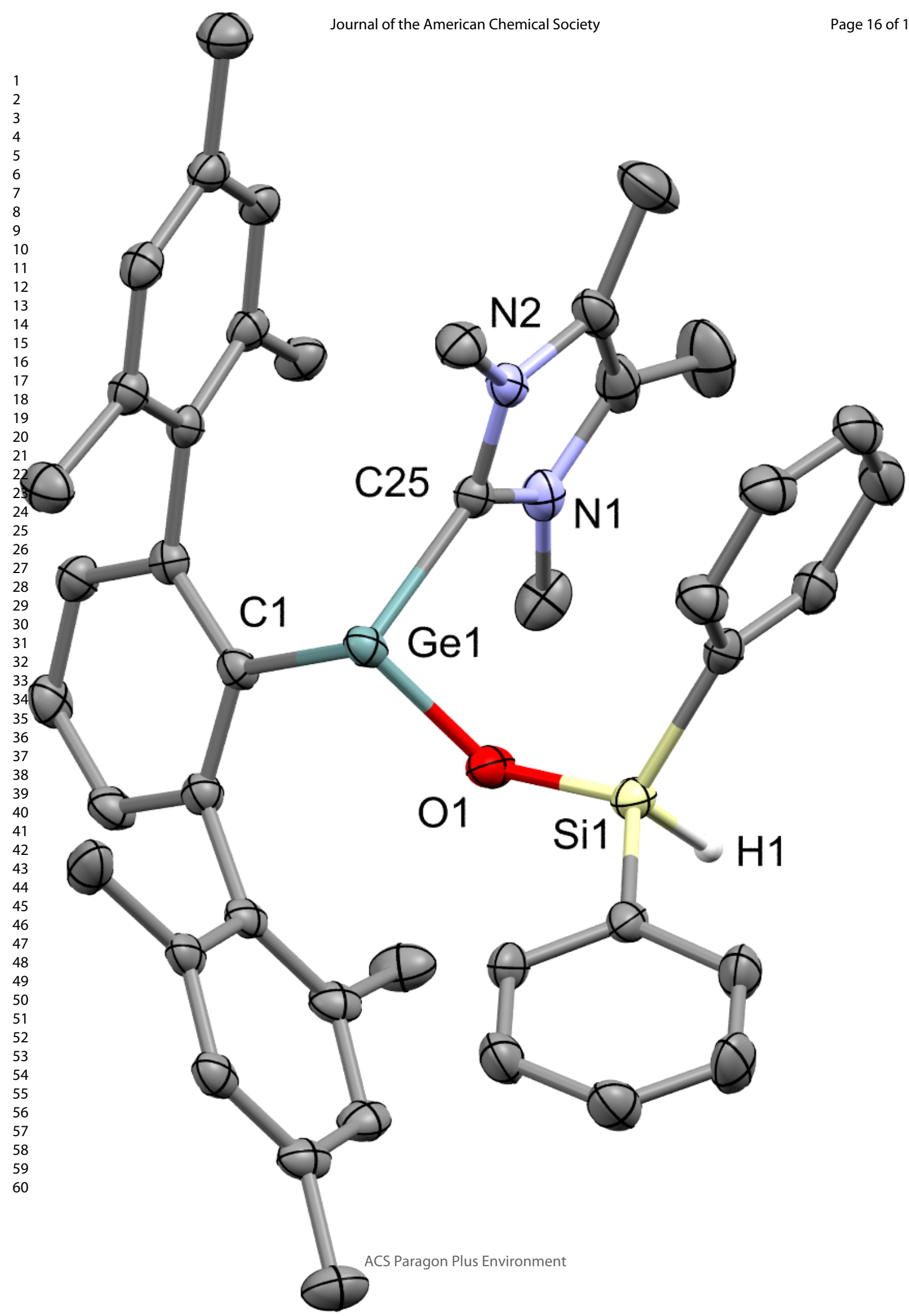
N2
C25
N1
C1
Ge1
O1
Si1
H1

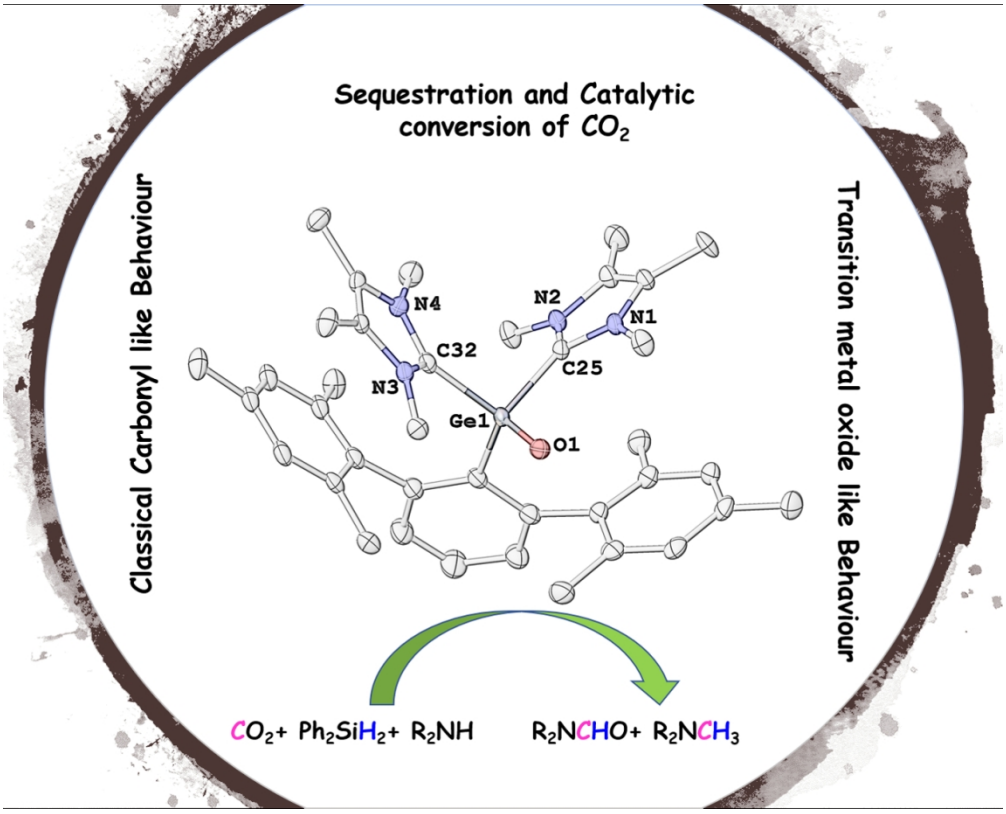

TOC

236x190mm (150 x 150 DPI)